Spectrochimica Acta Part A: Molecular and Biomolecular Spectroscopy 117 (2014) 587–597

Contents lists available at ScienceDirect

Spectrochimica Acta Part A: Molecular and Biomolecular Spectroscopy

journal homepage: www.elsevier.com/locate/saa

DFT calculations and electronic absorption spectra of some, α- and γ-pyrone derivatives

Walid M.I. Hassan [a], Hussein Moustafa [a,*], Mohamed N.H. Hamed [b], Laila I. Ali [b], Shimaa Abdel Halim [b]

[a] Chemistry Department, Faculty of Science, Cairo University, Giza, Egypt
[b] Chemistry Department, Faculty of Education, Ain Shams University, Cairo, Egypt

HIGHLIGHTS

- Electronic absorption spectra of α-, γ-pyrone and their derivatives were measured.
- The effects of solvent polarity on absorption spectra have been discussed.
- Energetics, donating and accepting power of the ground state were investigated.
- DFT calculations were used to theoretically assign experimental bands.

GRAPHICAL ABSTRACT

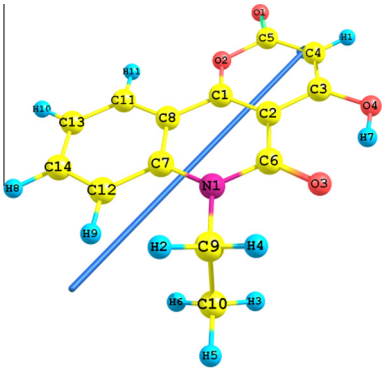

ARTICLE INFO

Article history:
Received 19 May 2013
Received in revised form 22 August 2013
Accepted 7 September 2013
Available online 19 September 2013

Keywords:
TD-DFT
Solvent effect
UV spectra
Alpha and gamma pyrone derivatives
MO-calculations

ABSTRACT

The electronic absorption spectra of 6-ethyl-4-hydroxy-2,5-dioxo-pyrano[3,2-c] quinoline **1**, 6-ethyl-4-hydroxy-3-nitro-2,5-dioxo-pyrano[3,2-c] quinoline **2**, 6-ethyl-4-chloro-2,5-dioxo-pyrano[3,2-c] quinoline **3**, 6-ethyl-3-nitro-4-chloro-2,5-dioxo-pyrano[3,2-c] quinoline **4**, 6-ethyl-4,5-dioxopyrano[3,2-c] quinoline **5**, and 6-ethyl-3-nitro-6H-pyrano [3,2-c]quinoline-4,5-dione **6**, were measured in polar (methanol) as well as nonpolar (dioxane) solvents. The geometries were optimized using B3LYB/6-311G (p,d) method. The most stable geometry of the studied compounds, **1**–**6**, is the planar structure as indicates by the values of the dihedral angles. The insertion of a nitro group in position 3 in both α- and γ-pyrone ring decreases the energy gap and hence increases the reactivity of **3** and **6** compounds. Assignment of the observed bands as localized, delocalized and/or of charge transfer (CT) has been facilitated by TD-DFT calculations. The correspondences between the calculated and experimental transition energies are satisfactory. The solvent and substituent effects have been investigated. Chloro-substituent has a higher band position and intensity effects on the spectra more than hydroxyl or nitro groups.

Introduction

Pyrone derivatives are a common fused heterocyclic nucleus found in many natural products of medicinal importance. Several of these natural products exhibit exceptional biological and pharmacological activities, such as antibiotic, antiviral, anti-HIV, anticoagulant and cytotoxicity properties [1–8]. Additionally, pyrone derivatives have been used as food additives, perfumes, cosmetics, dyes and herbicides [9,10]. The derivatives of 7-methyl-2H, 5H-pyrano [4,3-b] pyran-5-ones were used in vitro antiproliferative, cycto-toxic activity [11], and as anticancer activity against human tumor cell lines [12]. Derivatives of coumarins (benzo pyrone derivatives) were tested for wide toxicity drug. These compounds used as antileishmanial and antitrypanosomal activity of bufadienolides isolated from toad Rhinella jime parotoid macrogland secretion [13].

* Corresponding author. Tel.: +20 102589404.
E-mail address: hmamoustafa@hotmail.com (H. Moustafa).

1386-1425/$ - see front matter © 2013 Elsevier B.V. All rights reserved.
http://dx.doi.org/10.1016/j.saa.2013.09.057

The UV spectra of some α- and γ-pyrone derivatives were studied by Loakes et al. [14,15]. The results show that the lowest lying singlet excited state has n-π^* character, independent of the solvent used. The structural and vibrational spectroscopy data for the ground state demonstrated that no extensive π-system electron delocalization occurs in the pyrone moiety. Comparison of the spectroscopic results obtained for the monomeric species with those obtained for the room temperature condensed phase reveal that intermolecular interactions in these phases do not affect the structure and vibrational properties of pyrone derivatives [16].

Molecular orbital studies at the Huckle Molecular Orbital (HMO) level have been carried out on quinolines, α- and γ-pyrone derivatives [17]. More recently, the electronic structure calculations of some α- and γ-pyrone derivatives has been performed at

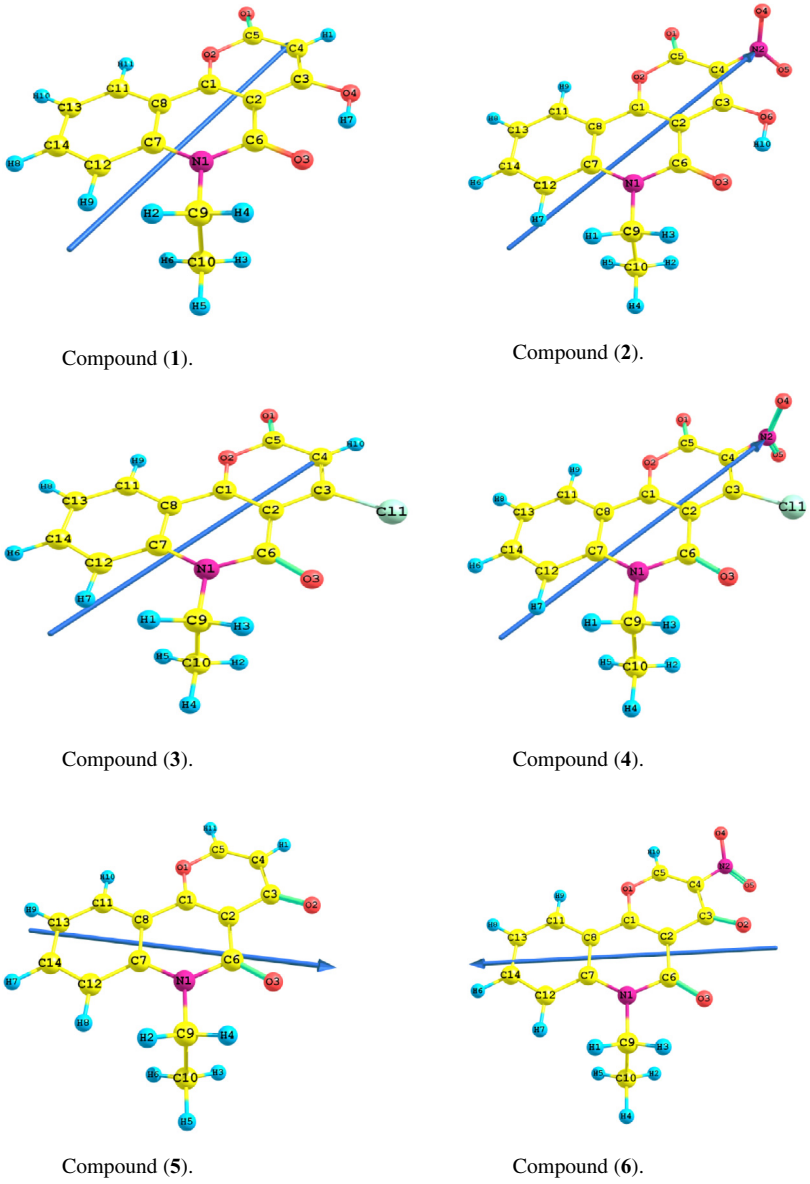

Compound (**1**). Compound (**2**). Compound (**3**). Compound (**4**). Compound (**5**). Compound (**6**).

Fig. 1. The optimized structure, perspective view of dipole moment of α- and γ-pyrone derivatives at B3LYP/6-311G (p,d).

Table 1
Total energy, energy of HOMO, LUMO, energy gap and dipole moment of compounds **1**–**6**.

G.S. properties	**1**	**2**	**3**	**4**	**5**	**6**
E_T (au)	−896.043	−1100.58	−1280.39	−1484.92	−820.752	−1025.29
E_{Homo} (eV)[a]	−6.4355	−6.9186	−6.5484	−6.8669	−6.3610	−6.7418
E_{Lumo} (eV)[b]	−2.3147	−2.8897	−2.5881	−3.0420	−2.0963	−2.7755
ΔE (eV)	4.1208	4.0289	3.9603	3.8249	4.2647	3.9663
μ (debye)	7.2563	11.8915	5.3601	9.3366	6.5381	9.8708

[a] I.E. = E_{Homo}.
[b] E.A = E_{Lumo}.

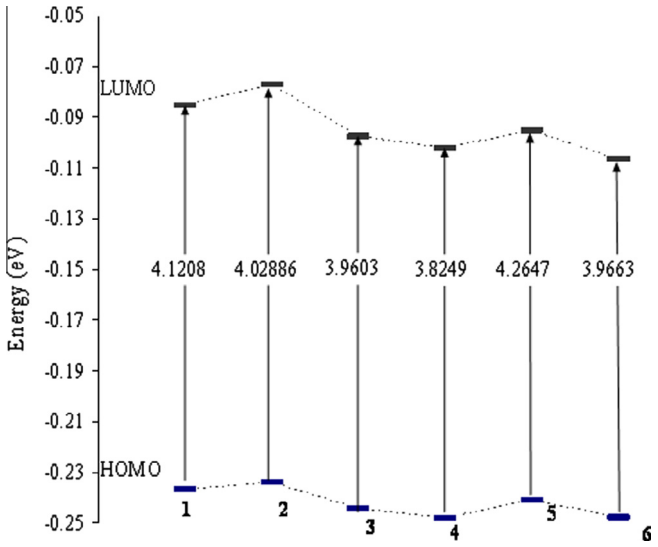

Fig. 2. Energy of HOMO, LUMO and energy gap of the studied compounds at B3LYP/6-311G (p,d) level of theory.

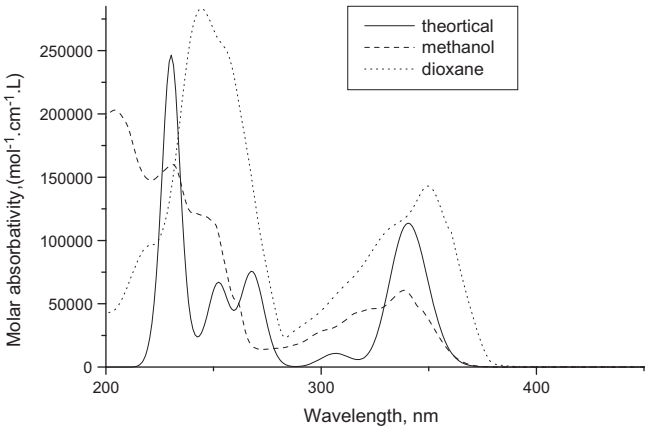

Fig. 3. Electronic absorption spectra of 1.

the RHF and DFT levels of theory [18,19]. The optimized geometry and ground state properties calculated using HF/6-31G*, are always smaller than those obtained by B3LYP/6-31G* and B3LYP/6-31 + G* methods.

The electronic structures of molecules usually manifest itself in the electronic absorption and emission spectra. This manifestation enables the detailed understanding of the forces that govern the electronic structure of the studied α-pyrone and γ-pyrones. Although, several investigations have been published that dealt with the electronic spectra of pyrones [20–23] yet there is no systematic study of substituents and solvent effects on the observed spectra. Such study is of critical importance in understanding their

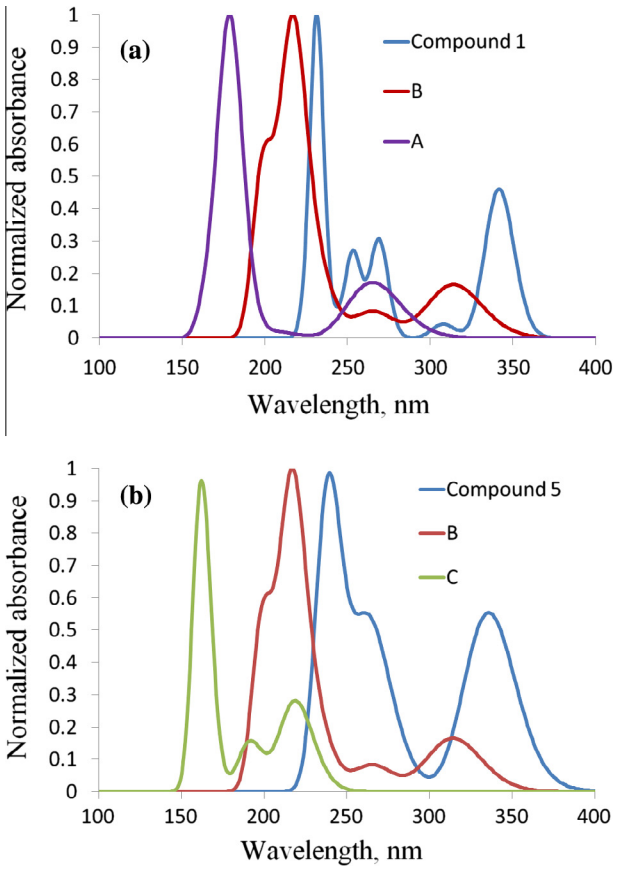

Fig. 4. Theoretical TD-DFT of (a) compound **1**, and (b) compound **5** and their subsystems.

electronic structure that might very well underline their biological activity.

The aim of our work is (i) to explore the ground state properties of the studied α- and γ-pyrone derivatives at the density functional level of theory (DFT) method using B3LYP/6-311G**, (ii) the type and extent of conjugative interaction between different subsystems of α-pyrone and γ-pyrone, (iii) the effect of solvent polarity on the observed spectra and hence, predicting the relative stabilities, extent of charge transfer character and assignment of the observed electronic transitions, and (iv) the effect of different substituents, on the electronic spectra of α- and γ-pyrone derivatives.

Experimental

Compounds

The compounds studied were prepared and purified using standard procedures cited in the literature [24]. Below, is shown the different pyrones used in this study, where compound **1** is 6-ethyl-4-hydroxy-2,5-dioxo-pyrano[3,2-c]quinoline, **2** is

Table 2
TD-DFT electronic absorption band for α- and γ-pyrone and N-ethyl-quinoline.

State	α-Pyrone (**A**-moiety)	γ-Pyrone (**C**-moiety)	N-Et-quinoline-2-one (**B**-moiety)
I	265.01	225.22	314.33
II	179.14	217.85	265.03
III	168.33	191.49	233.42
IV	165.97	164.35	220.14
V		161.66	217.00
VI			213.37

6-ethyl-4-hydroxy-3-nitro-2,5-dioxo-pyrano[3,2-c]quinoline, **3** is 6-ethyl-4-chloro-2,5-dioxo-pyrano[3,2-c]quinoline, **4** is 6-ethyl-3-nitro-4-chloro-2,5-dioxo-pyrano[3,2-c]quinoline, **5** is 6-ethyl-4,5-dioxopyrano[3,2-c]quinoline, and **6** is 6-ethyl-3-nitro-6H-pyrano (3,2-c)quinoline-4,5-dione; as shown in Fig. 1.

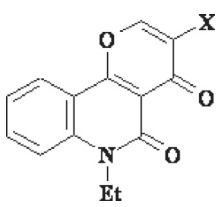

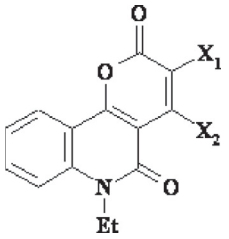

γ-Compounds	X
5	H
6	NO_2

α-Compounds	X_1	X_2
1	H	OH
2	NO_2	OH
3	H	Cl
4	NO_2	Cl

Solvents

Polar (methanol) and non-polar (dioxane) solvents were obtained from Merck, AR-grade, and were used without further purification.

Apparatus

The electronic absorption spectra were measured using a Perkin Elmer lambda 4B spectrophotometer using 1.0 cm fused quartz cells. The machine records linearly the percent of transmittance over the range 200–700 nm.

Computational details

In this work, DFT (B3LYP) [18] method were used. This function is a combination of the Becke's three parameters non-local exchange potential with the non-local correlation functional of Lee et al. Full geometry optimization was performed using 6-311G (p,d) [19] as a basis set to generate the optimized structures and ground state properties of the studied α- and γ-pyrone derivatives. The electronic transition properties which include the maximum excitation wavelength (λ_{max}) and relative intensities (oscillator strengths, *f*), were obtained by the time dependant density functional theory (TD-DFT), [18]. All calculations were performed using Gaussian 09W program package [25].

Result and discussion

Ground state properties

Optimized structures of the all molecules obtained using the B3LYB/6-311G (p,d) level are presented in Fig. 1. The energies of HOMO, LUMO, energy gap and dipole moment of all derivatives are presented in Fig. 2 and Table 1. Analysis of Table 1 and Fig. 2 show that:

- The most stable geometry of the studied compounds, **1**–**6**, is the planar structure, (add dihedral angle) which means that the two moieties, α- or γ-ring (**A**- or **C**-moiety) and N-ethyl-quinoline (NQ) (**B**-moiety) is in the same molecular plane. The insertion of Cl-atom in position 4 or nitro group in position 3 does not change the planarity of compounds.
- The ionization energy, I.E., of compound **1** which measures the donating property (oxidation power) is 6.43 eV (c.f. Table 1). Introducing a nitro-group in position 3, of compound **1** results in the formation of compound **2,** similarly replacing a hydroxyl group of compound **1** by a Cl-atom, produces compound **3,** the introduction of a nitro-group in position 3, in compound **1** and

Table 3
Calculated band maxima and intensities of compound **1** by TD method.

State	Theoretical					Experimental	
	Configuration	Coefficient	λ (nm)	*f*	Type	Polar λ (nm)	Nonpolar λ (nm)
I	67–68	0.69340	341.50	0.1545	π–π*	340.22	350.20
II	66–68	0.67369	310.23	0.0703	π–π*	317.73	330.83
	67–68	0.15373					
III	62–68	0.10470	268.89	0.1019	π–π*	297.70	282.67
	65–68	0.40817					
	67–69	0.54945					
IV	62–68	−0.10991	253.58	0.0765	π–π*	259.53	257.66
	63–68	−0.24393					
	65–68	0.40966					
	66–69	−0.33212					
	67–69	−0.31312					
	67–70	0.12189					
V	63–68	0.64652	251.60	0.1708	π–π*	250.14	243.91
	65–68	0.16782					
	66–69	−0.11513					
	67–69	−0.12090					
VI	61–68	0.11639	224.94	0.3233	π–π*	230.76	216.37
	62–68	0.47133					
	64–69	0.15367					
	66–69	0.11131					
	66–70	0.17891					
	66–71	0.10207					
	67–70	−0.27495			π–π*		
	67–71	0.30776			π–π*		

simultaneously replacing OH group in position 4 by a Cl-atom, produces compound **4.** Such substituent effect shows a significant change in the I.E. and hence in the donating properties. Accordingly, one can put the order of decreasing the donating power is **1** > **3** > **4** > **2**.

- However the electron affinity, E.A., of **1** which measures the accepting property (reducing power) is 2.314 eV. The order of accepting properties of α-derivatives follows **1** < **3** < **2** < **4**. In the case of γ-derivatives, for compound **5**, the electron affinity, E.A., is 2.096 eV and the I.E. is 6.36 eV. Introducing a nitro-group in position 3, in compound **5** results in the formation of compound **6** where such modification shows a significant change in the I.E. and E.A. following the order **5** < **6**.
- The band gaps in the pyrone derivatives **1**–**6** are governed by their chemical structures. The calculated band gap Δ*E* of α-pyrone derivatives decreases in the following order: **1** > **2** > **3** > **4** and **5** > **6** in case of γ-derivatives. This indicates that the lower the Δ*E*, the higher the reactivity of these compounds.
- Finally, the theoretically computed dipole moment for compound **1** is 7.25 D. The Insertions of a nitro-group in position 3 increases the dipole moment in α- and γ-derivatives and follows the order **2** > **1** and **6** > **5** (c.f. Table 1**).** On the other hand, replacing the OH group of compound **1** by a Cl-atom**,** (compound **3),** decreases the value of the dipole moment**.** The general trend of the dipole moment for the studied α-derivatives follows the order **2** > **4** > **1** > **3**.

Electronic absorption spectra

The electronic absorption spectra of α- and γ-pyrone derivatives studied in this work **1**–**6** depend on the type and extent of interaction between different moieties. Two possible types of interaction between subsystems indicate the following:

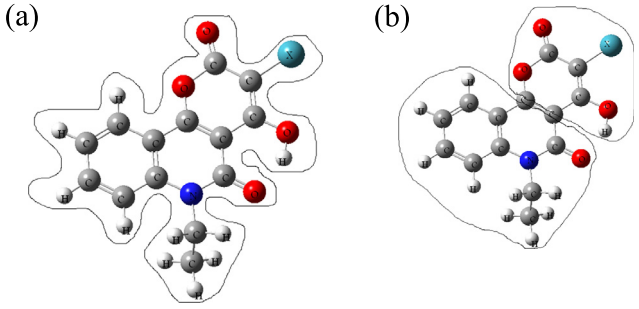

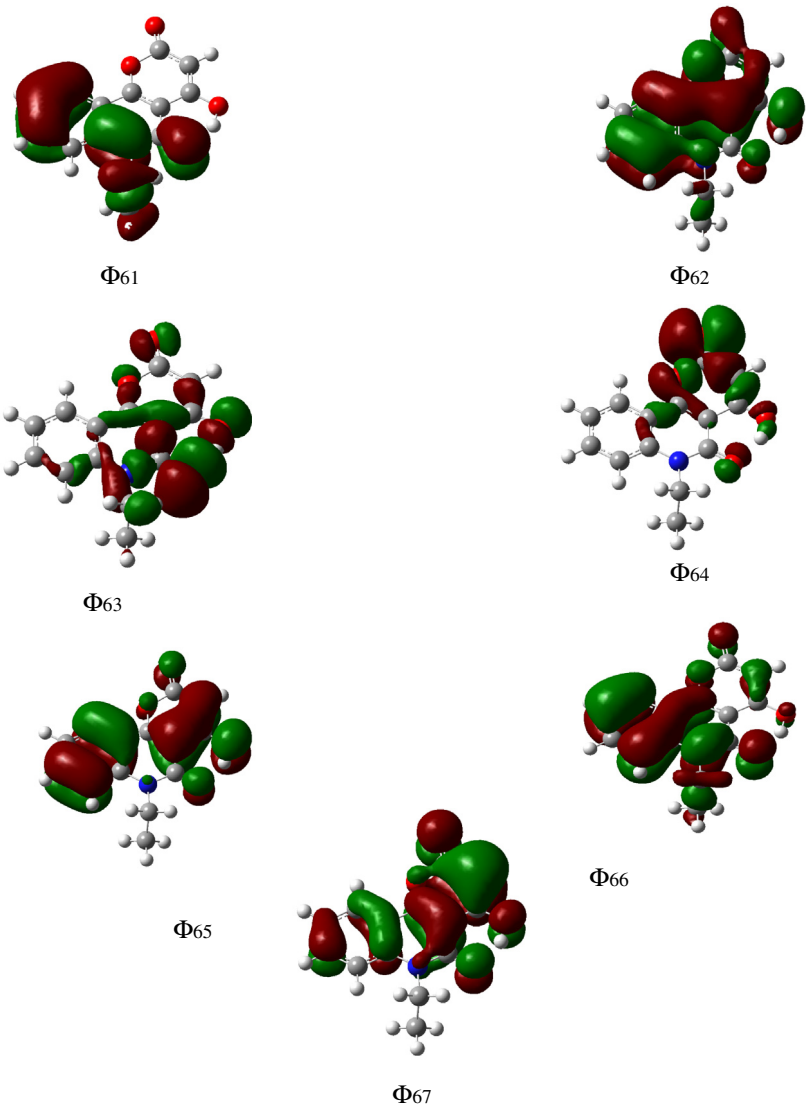

Fig. 5. The charge density maps of the occupied MO's for compound **1**.

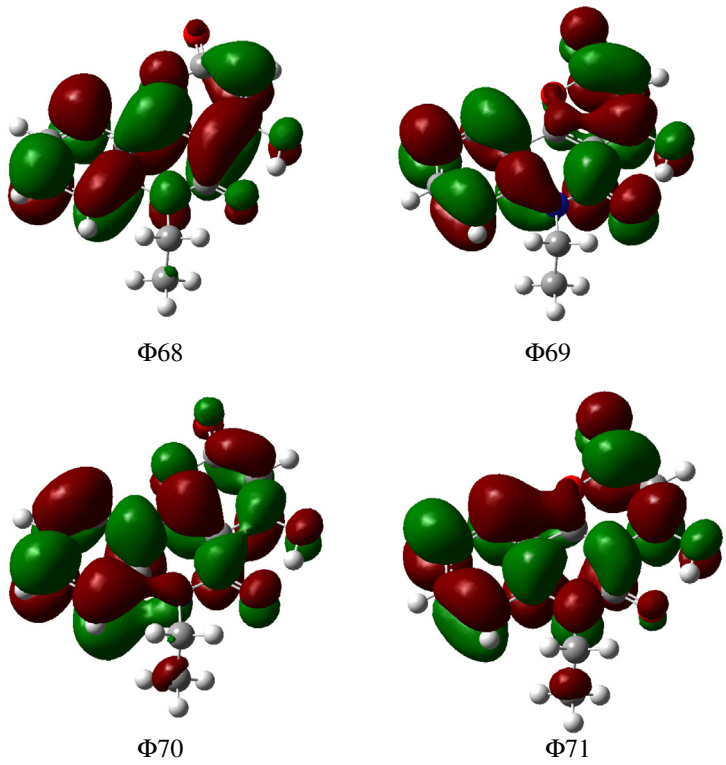

Fig. 6. The charge density maps of the unoccupied MO's. for compound **1**.

Full conjugation which extends over the whole molecule (a) reflects that the spectrum of α- or γ-pyrone and their derivatives should be completely different from that of its subsystems. Partial or cross-conjugation (b) reflects that the spectrum of α- and γ-pyrone derivatives are additive spectra.

Electronic absorption spectra of α-pyrone and its derivatives

The electronic absorption spectrum of compound **1** in methanol and dioxane are presented in Fig. 3. The spectrum is composed of 6 bands spanning the range 215–360 nm. Due to the complexity of the spectrum of compound **1**, we calculate the theoretical transitions of its subsystems, viz., **A**-moiety and **B**-moiety. The theoretical calculations of the subsystems can help in predicting the origin of the observed spectra of compound **1**. The theoretical electronic transitions and the theoretical spectra are presented in Table 2 and Fig. 4a. The theoretical spectra of the subsystems of compound **1**, namely, 4-hydroxy 2-pyrone (**A**) and ethyl quinoline 2-one (NQ) (**B**), are presented in Fig. 4a. Analysis of Fig. 4a and Table 2 show that.

For α-pyrone moiety (**A**), the main band computed theoretically is centered at 265 nm and for **B**, four bands computed theoretically centered at 314 nm, 265 nm, 233 nm and 220 nm. The observed spectra of compound **1** in dioxane as shown in Table 3 are composed of 6-bands centered at 350.20 nm, 330.83 nm, 282.67 nm, 257.66 nm, 243.91 nm and 216.37 nm. The bands of **A** and **B** moieties computed theoretically are not found in the observed spectra of compound **1** indicating that a conjugative interaction between the two subsystems structure (a) is expected and hence new spectrum is observed (c.f. Fig. 3). Increasing the solvent polarity on going from dioxane to methanol causes change in band positions and marked decrease in the intensity of all bands. All the observed bands may be assigned to (π–π^*) transitions as reflected from their intensities (40.000–250.000).

Excited configurations, considered in compound **1**, are those which results from an electron excitation of seven highest occupied molecular orbital's $\varphi_{61}^{-1}\varphi_{67}$ and the lowest four unoccupied molecular orbital's $\varphi_{68}^{-1}\varphi_{71}$. The configurations interaction matrix is solved and the configurations interaction state functions are given in Table 3 and Figs. 5 and 6. All computed transitions at TD/DFT/B3LYP/6-311G** level are in agreement with the observed transitions in methanol and dioxane solvents.

The long wavelength absorption band has been computed theoretically at 341.5 nm and composed of one configuration, $\varphi_{67}^{-1}\varphi_{68}$, with oscillator strength 0.154. This band shows a blue shift on increasing solvent polarity, that is, solvent dependence. This may be attributed to the relatively high polarity of the excited state as compared to that of the ground state. This state may be assigned as a delocalized transition (c.f. Figs. 5 and 6). The second (π–π^*)[1]

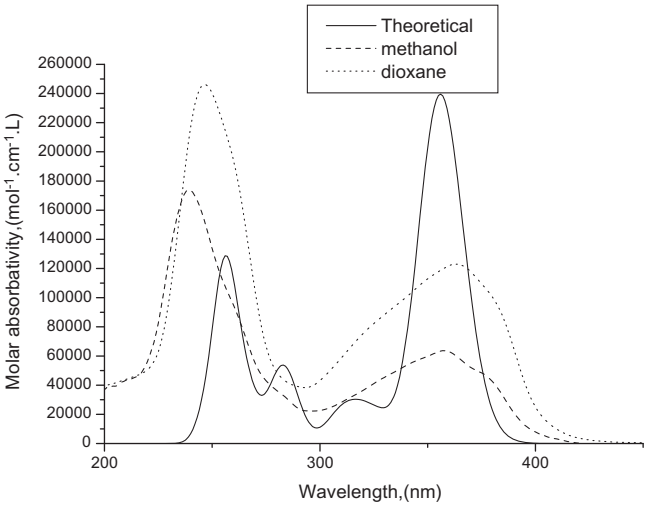

Fig. 7. Electronic absorption spectra of compound **2**.

Table 4
Calculated band maxima and intensities of compound **2** by TD method.

State	Theoretical					Experimental	
	Configuration	Coefficient	λ (nm)	f	Type	Polar λ (nm)	Nonpolar λ (nm)
I	76–80	0.10557	355.94	0.2131	π–π^*	359.6	364.1
	78–79	0.65289					
	78–80	0.12739					
	78–81	0.13302					
II	73–79	0.10223	310.89	0.0198	π–π^*	315	320
	76–79	−0.15679					
	76–80	−0.18042					
	76–81	−0.13361					
	77–79	0.38862					
	77–80	−0.11591					
	78–79	0.22066					
	78–80	−0.30670					
	78–81	−0.28607				275	281
III	75–79	−0.21752	283.07	0.0471	π–π^*		
	76–79	0.48675					
	78–80	−0.38935					
IV	70–79	0.14379	256.10	0.0973	π–π^*		247.1
	72–79	−0.19956				240.1	
	73–79	0.25201					
	75–79	−0.13634					
	76–79	0.22148					
	76–80	−0.10987					
	77–80	0.27940					
	77–81	−0.21228					
	78–80	0.23319					
	78–81	−0.24253					

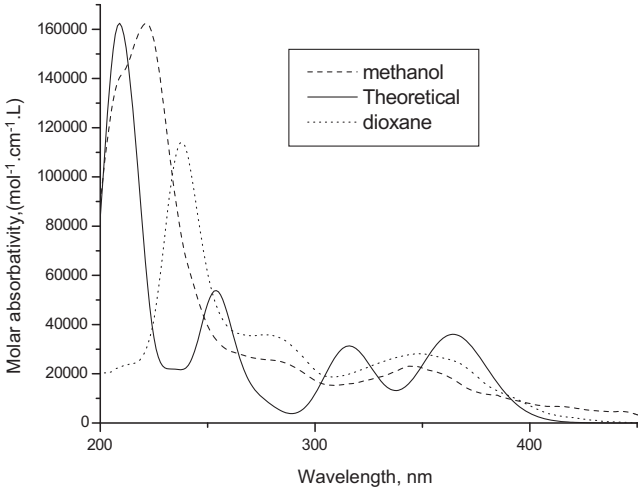

Fig. 8. Electronic absorption spectra of compound **3**.

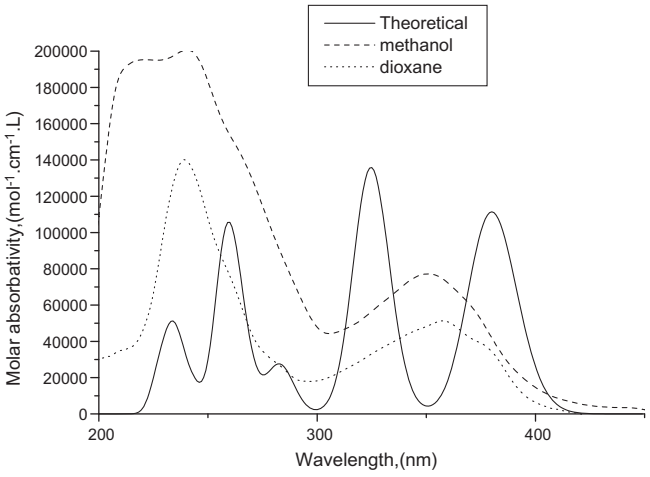

Fig. 9. Electronic absorption spectra of compound **4**.

state is computed theoretically at 310.2 nm. This state is composed of two configurations, namely, $\varphi_{66}^{-1}\varphi_{68}$, $\varphi_{67}^{-1}\varphi_{68}$. This band shows a blue shift on increasing solvent polarity, that is, solvent dependent. The first configuration which represents the main contribution of this state ($\varphi_{66}^{-1}\varphi_{68}$) is a localized band where, the second configuration ($\varphi_{67}^{-1}\varphi_{68}$) may be assigned as a delocalized transition (c.f. Figs. 5 and 6). The third $(\pi$–$\pi^*)^1$ state observed at 283 nm in dioxane, 297 nm in methanol and computed theoretically at 269 nm. This state possesses a high polarity as compared to the ground state and hence solvent dependent, accompanied by a change in band position (≈15 nm). This state is composed of three configurations, namely, ($\varphi_{62}^{-1}\varphi_{68}$, $\varphi_{65}^{-1}\varphi_{68}$ and $\varphi_{67}^{-1}\varphi_{69}$. Both configurations $\varphi_{62}^{-1}\varphi_{68}$ and $\varphi_{67}^{-1}\varphi_{69}$ are (CT) bands from the **B**-moiety to the **A**-moiety, where, the configuration $\varphi_{65}^{-1}\varphi_{68}$ is a delocalized band. The fourth $(\pi$–$\pi^*)^1$ state is computed theoretically at 254 nm. This state is composed of six configurations, namely, $\varphi_{62}^{-1}\varphi_{68}$, $\varphi_{63}^{-1}\varphi_{68}$, $\varphi_{65}^{-1}\varphi_{68}$, $\varphi_{66}^{-1}\varphi_{69}$, $\varphi_{67}^{-1}\varphi_{69}$ and $\varphi_{67}^{-1}\varphi_{70}$. This state shows no solvent dependent. The configurations $\varphi_{62}^{-1}\varphi_{68}$, $\varphi_{66}^{-1}\varphi_{69}$ and $\varphi_{67}^{-1}\varphi_{69}$ may be assigned as (CT) bands from the **B**-moiety to the **A**-moiety, where, the configurations $\varphi_{65}^{-1}\varphi_{68}$ and $\varphi_{63}^{-1}\varphi_{68}$ may be assigned as delocalized bands, and the configurations $\varphi_{67}^{-1}\varphi_{70}$ assigned as (CT) bands from the **B**-moiety to the **A**-moiety. The overall contribution of this state may be assigned as (CT) band from the **B**-moiety to the **A**-moiety as indicated by the coefficient of their

Table 5
Calculated band maxima and intensities of compound **3** by TD method.

State	Theoretical					Experimental	
	Configuration	Coefficient	λ (nm)	f	Type	Polar λ (nm)	Nonpolar λ (nm)
I	70–72	0.15879	364.34	0.1399	π–π^*	365.7	367.6
	71–72	0.68138					
II	69–72	−0.12998	316.11	0.1186	π–π^*	344.6	348.5
	70–72	0.66291					
	71–72	−0.15657					
III	68–72	−0.38146	253.98	0.1364	π–π^*	285.2	283.9
	69–73	0.30217					
	70–73	0.45094					
	70 – 74	−0.10553					
	71–73	0.15273					
IV	65–72	−0.21003	215.98	0.2545	π–π^*	221.7	237.6
	66–72	0.28733					
	68–74	−0.23134					
	70–73	0.15077					
	71–73	−0.14673					
	71–74	−0.22223					
	71–75	0.43221					
V	65–72	−0.31945	207.28	0.4213	π–π^*	208.4	210.7
	66–73	0.10700					
	68–72	−0.13832					
	68–73	0.34963					
	68–74	−0.11026					
	69–74	0.16499					
	70–74	0.37215					
	71–73	0.11525					

Table 6
Calculated band maxima and intensities of compound **4** by TD method.

State	Theoretical					Experimental	
	Configuration	Coefficient	λ (nm)	f	Type	Polar λ (nm)	Nonpolar λ (nm)
I	81–83	0.14376	379.99	0.1493	π–π^*	373.9	377.7
	82–83	0.68605					
II	80–83	−0.11689	324.82	0.1802	π–π^*	350.8	358.9
	81–83	0.66512					
	82–83	−0.14327					
III	79–83	−0.24334	283.05	0.0355	π–π^*	268.9	279.5
	82–85	0.63293					
IV	74–83	0.11884	257.41	0.0850	π–π^*	242.1	257.1
	77–83	0.11447					
	79–83	−0.28060					
	80–85	0.21515					
	81–85	0.50195					
	82–86	0.22984					
V	73–83	0.17297	234.39	0.0553	π–π^*	215.8	240.7
	81–85	−0.12478					
	81–86	−0.31730					
	81–87	0.12050					
	82–86	0.49306					
	82–87	0.24257					

configurations. The fifth $(\pi$–$\pi^*)^1$ state is computed theoretically at 252 nm and composed of four configurations with oscillator strength 0.1708. This state shows no solvent dependent and assigned as delocalized band. The last state computed theoretically appears at 225 nm with oscillator strength 0.323. Increasing the solvent polarity results in a red shift, that is, a solvent dependent. This state is composed of eight configurations (c.f. Table 3) and may be assigned as CT bands from the **B**-moiety to the **A**-moiety (c.f. Figs. 5 and 6).

Insertion of a nitro group in position 3 of compound **1** gives compound **2**. The electronic spectra of compound **2** in methanol and dioxane solvents, assignment of spectra are given in Fig. 7 and Table 4. The spectrum in dioxane is composed of four bands centered at 364 nm, 320 nm, 281 nm and 247 nm. Increasing solvent polarity on going from dioxane to methanol causes small changes in band positions indicating that the polarity of the excited and ground state are of the same values, that is, solvent independent. The intensity is lowered in methanol and all bands are

Table 7
Calculated band maxima and intensities of compound **5** by TD method.

State	Theoretical					Experimental	
	Configuration	Coefficient	λ (nm)	f	Type	Polar λ (nm)	Nonpolar λ (nm)
I	62–64	−0.3739	335.67	0.1053	π–π^*	340.5	351.5
	62–65	−0.1166					
	63–64	0.57209					
II	59–64	0.24956	259.93	0.0668	π–π^*	240.8	263.3
	60–64	0.59559					
	63–66	0.23676					
III	59–65	0.27324	240.73	0.0542	π–π^*	233.3	239.5
	60–65	−0.21979					
	61–65	0.42465					
	62–66	−0.36090					
	63–66	−0.21745					
IV	59–65	−0.37635	238.17	0.1325	π–π^*	212.8	215.8
	61–65	0.49269					
	62–66	0.24150					
	63–66	0.14724					

assigned to (π–π^*) transitions as reflected from their intensities (40.000–250.000). The excited configurations considered in compound **2** are those which results from an electron excitation of nine highest occupied molecular orbital's $\varphi_{70}^{-1}\varphi_{78}$ and the lowest three vacant molecular orbital's $\varphi_{79}^{-1}\varphi_{81}$. The correspondence between the theoretically computed and the experimentally observed transitions are satisfactory.

If OH group in position 4 of compound **1** is replaced by a Cl-atom, iso-electronic compound **3** is obtained. Cl-atom is an electron donor by its mesomeric effect and is an electron acceptor by its inductive effect. Fig. 8 presents the electronic absorption spectra of compound **3** in methanol and dioxane solvents with the theoretical spectra. The state energies coefficient of each configuration, assignment, type of electronic transitions, theoretically computed and experimentally observed wavelengths are given in Table 5. The general feature of the spectrum appears different from the spectrum of compound **1**. The spectrum in dioxane shows five bands centered at 368, 349, 284, 238 and 211 nm. Increasing solvent polarity, on going from dioxane to methanol, decreases the intensities of all bands with a blue shift of the band at 238 in dioxane to 222 nm in methanol (≈16 nm).

To complete our investigation of substituent effect on the electronic structure and spectra of compound **1**, we introduce a Cl-atom in position 4 and a nitro group in position 3. Fig. 9 and Table 6 present the spectra of compound **4** in methanol and dioxane solvents with the theoretical spectra. The spectrum is composite and does not correspond to any one of its subsystems, which indicates a considerable conjugative interaction between them. The general feature of the spectrum is the same as compound **2** and compound **3** in band positions with lowering in the intensity of these bands. The spectrum in dioxane is composed of five bands centered at 378 nm, 359 nm, 279 nm, 257 nm and 241 nm. Increasing solvent polarity on going from dioxane to methanol increases the intensity of all bands with a blue shift of all bands except the long wavelength band. All observed bands are (π–π^*) transitions as indicated from their intensities (40.000–200.000). The excited configurations considered in compound **4** are those which results from an electron excitation of ten highest occupied molecular orbital's $\varphi_{73}^{-1}\varphi_{82}$ and the lowest five vacant orbital's $\varphi_{83}^{-1}\varphi_{87}$.

Electronic absorption spectra of γ-pyrone and its derivatives

The spectrum of the π-isoelectronic molecule of compound **5** is presented in Fig. 10 in methanol and dioxane solvents. The general feature of the spectrum appears different from that of compound **1**. The difference in spectra can be attributed to the difference in the

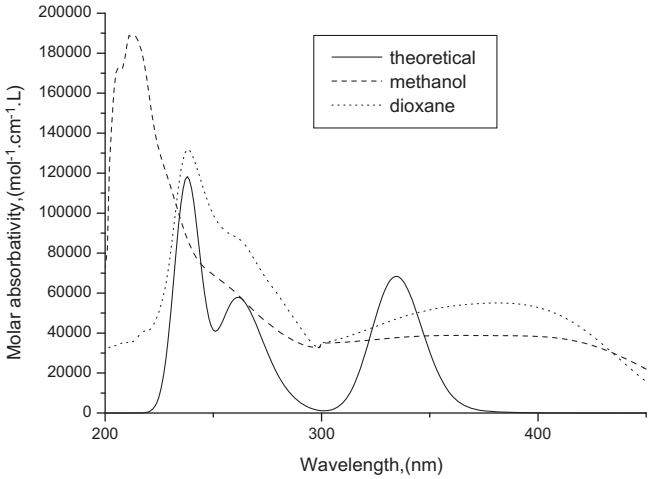

Fig. 10. Electronic absorption spectra of compound **5**.

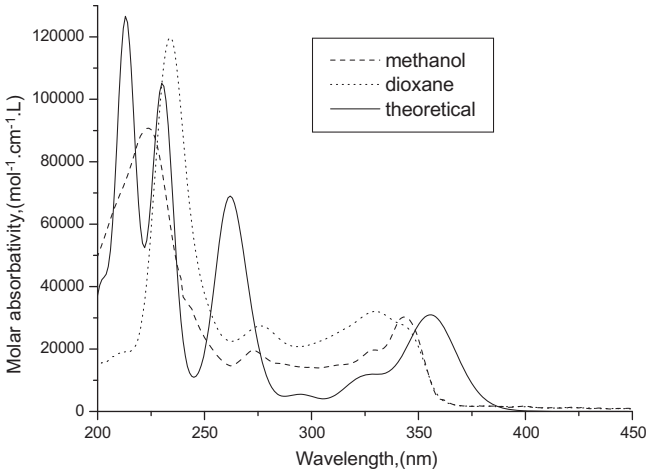

Fig. 11. Electronic absorption spectra of compound **6**.

structure of the C-moiety (c.f. Table 2). Therefore, it is not plausible to compare the spectra of compounds **1** and **5**. The theoretical spectrum of the two subsystems of **5**, via, C-moiety and B-moiety is presented in Table 2 and Fig. 4b. The observed spectrum of com-

Table 8
Calculated band maxima and intensities of compound **6** by TD method.

State	Theoretical					Experimental	
	Configuration	Coefficient	λ (nm)	f	Type	Polar λ (nm)	Nonpolar λ (nm)
I	73–75	−0.3362	357.01	0.0882	π–π^*	347.1	345.8
	73–76	0.20881					
	74–75	0.53740					
	74–76	0.17783					
II	72–76	0.56476	270.10	0.0552	π–π^*	327.7	332.7
	73–77	−0.13419					
	74–77	0.35645					
III	67–75	0.21400			π–π^*	275.7	278.3
	67–76	−0.11073	263.23	0.0895			
	68–75	0.16753					
	69–75	−0.29850					
	70–76	−0.20319					
	71–75	0.42735					
	71–76	0.21684					
IV	69–76	−0.31700	231.33	0.1616	π–π^*	239.5	233.9
	70–77	0.18434					
	71–77	−0.22645					
	72–75	0.10988					
	72–76	0.11029					
	72–78	0.12425					
	74–78	0.40624					
	74–79	0.25963					
V	66–75	0.22784	214.46	0.2619	π–π^*	223.8	210.8
	67–76	−0.16024					
	69–77	−0.15341					
	70–77	−0.10285					
	72–77	0.11761					
	73–79	0.23864					
	74–78	−0.25155					
	74–79	0.42721					

pound **5** is composite and does not correspond to any one of its subsystems, which indicate a considerable conjugative interaction between them. The intensity of the observed bands of compound **5** is decreased (≈40.000–200.000). All the observed bands are (π–π^*) transitions as reflected from their intensities. The spectrum in dioxane is composed of four bands centered at 351 nm, 263 nm, 239 nm and 216 nm. Increasing solvent polarity shows a blue shift in the long wavelength absorption band and increases the intensity. Excited configurations considered in compound **5** are those which results from an electron excitation of five highest occupied molecular orbital's $\varphi_{59}^{-1}\varphi_{63}$ and lowest three vacant molecular orbital's $\varphi_{64}^{-1}\varphi_{66}$.

The first $(\pi$–$\pi^*)^1$ state computed theoretically at 335 nm and observed at 351 nm in dioxane. This band shows a blue shift (≈10 nm) (c.f. Table 7) on going from dioxane to methanol and composed of a mixture of three configurations, namely, $\varphi_{62}^{-1}\varphi_{64}$, $\varphi_{62}^{-1}\varphi_{65}$ and $\varphi_{63}^{-1}\varphi_{64}$. The main contribution of this band is coming from $\varphi_{63}^{-1}\varphi_{64}$ which is (CT) band from the B-moiety to the C-moiety. The second $(\pi$–$\pi^*)^1$ state is observed at 263 nm in dioxane and shows a solvent dependent (blue-shift) on going from dioxane to methanol by 23 nm. This band is composed of three configurations (c.f. Table 7) and is (CT) band from the B-moiety to the C-moiety. The last two bands show no solvent dependent and both are of (CT) band from the B-moiety to the C-moiety (c.f. Table 7).

Fig. 11 and Table 8 present the spectra of compound **6** in methanol and dioxane solvents with the theoretical spectra. The long wavelength envelope of the spectrum is broad and diffuses. The insertion of nitro-group is position 3 of the C-moiety decreases the intensity of all observed bands and two new bands appears under this envelope. The molecular orbital considered in the electronic transition of compound **6** are nine occupied molecular orbital's $\varphi_{66}^{-1}\varphi_{74}$ and five vacant molecular orbital's $\varphi_{75}^{-1}\varphi_{79}$. All the observed transitions may be assigned as (π–π^*) as reflected from their intensities. The spectrum in dioxane shows five bands centered at 346 nm, 332 nm, 278 nm, 234 nm and 211 nm. Increasing solvent polarity shows no solvent dependent.

Summary and conclusion

The most stable geometry at B3LYB/6-311G (p,d) level of the studied compounds, **1**–**6**, is the planar structure. The two moieties, **A** or **C** and **B** moieties are in the same molecular plane. The insertion of Cl-atom in position 4 or nitro group in position 3 in compound **1** does not change the planarity of the compounds. The band gaps in pyrones derivatives **1**–**6** are governed by their chemical structures. The calculated band gap ΔE decreases in the following order: **1** > **2** > **3** > **4** in case of α-derivatives and **5** > **6** in case of γ-derivatives. The much lower the ΔE indicates a significant effect of the intermolecular charge transfer and hence increases the reactivity of the compounds. The general trend of the dipole moment computed theoretically for the studied α-derivatives follows the order **2** > **4** > **1** > **3** and for γ-derivatives **6** > **5.**

The electronic absorption spectra of α- and γ-pyrone derivatives studied in this work **1**–**6** depend on the type and extent of interaction between different moieties. Full conjugation which extends over the whole molecule reflects that the spectrum of α- or γ-pyrone and their derivatives should be completely different from that of its subsystems.

All the observed bands can be assigned to (π–π^*) transitions as reflected from their intensities. The correspondence between the

theoretically computed and the experimentally observed transitions are satisfactory. The solvent dependence of the observed bands can be attributed to the charge in the dipole moments of the ground and excited states.

References

[1] R.D.H. Murray, J. Mendez, S.A. Brown, The Natural Coumarins: Occurrence Chemistry and Biochemistry, Wiley & Sons, New York, NY, USA, 1982.
[2] B. Naser-Hijazi, B. Stolze, K.S. Zanker, in: 2nd Proceedings of the International Society of Coumarin Investigators, Springer, Berlin, Germany, 1994.
[3] R. OKennedy, R.D. Thornes, Coumarins: Biology Applications and Mode of Action, Wiley & Sons, Chichester, UK, 1997.
[4] J.D. Hepworth, in: A. Katritzky, C.W. Rees, A.J. Boulton, A. Mekillop (Eds.), Comprehensive Heterocyclic Chemistry, vol. 3, Pergamon Press, Oxford, UK, 1984, p. 799.
[5] J.C. Jung, Y.J. Jung, O.S. Park, A Convenient one-pot synthesis of 4-hydroxycoumarin, 4-hydroxythiocoumarin and 4-hydroxyquinolin-2(1H)-one, Synth. Commun. 31 (2001) 1195.
[6] C. Gnerre, M. Catto, F. Leonetti, P. Weber, P.A. Carrupt, C. Altomare, A. Carotti, B. Testa, Inhibition of monoamine oxidases by functionalized coumarin derivatives: biological activities, QSARs, and 3D-QSARs, J. Med. Chem. 43 (2000) 4747.
[7] M. Zahradnik, The Production and Application of Fluoroscent Brightening Agents, Wiley & Sons, New York, NY, USA, 1982.
[8] S. Hesse, G. Kirsch, Tetrahedron Lett. 43 (2002) 1213.
[9] L.A. Singer, N.P. Kong, J. Am. Chem. Soc. 88 (1966) 5213.
[10] S. Carboni, V. Malaguzzi, A. Marzili, Tetrahedron Lett. 5 (1964) 2783.
[11] A. Lawrence, D. Willians, Heiko Leutbecher, Harald Rosner, Uwe Beifuss, Bioorg. Med. Chem. L 17 (2007) 978.
[12] G. Hartinger Christian, A. Nazarror Alexey, Wolfgang Kandioller, Jahanna Kasser, Roland John, A. Jakapec Micheal, B. Arion Vladimir, J. Dyson Poul, Bernhardk Keppler, J. Org. Chem. 694 (2009) 922.
[13] A.G. Tempone, D.C. Pimenta, I. Lebrun, P. Sartorelli, N.N. Taniwaki, H.F. de Andrade Jr., M.M. Antoniazzi, C. Jared, Toxicon 52 (2008) 13.
[14] P.S. Soon, W.H. Gordon, J. Phys. Chem. 74 (1970) 4234.
[15] D. Loakes, D.M. Brown, S.A. Salisbury, J. Chem. Soc. Perkins Trans. 1 (1999) 1333.
[16] R. Fausto, G. Quinteino, S. Breda, J. Mol. Strct. 598 (2001) 287.
[17] A.R. Jorge, M.A. Remero, J.M. Salas, M. El-Bahraoui, J. Molina, J. Inorg. Chem. 35 (1996) 7829.
[18] J.G. Matecki, Trans. Met. Chem. 35 (2010) 801.
[19] W.Y. Lee, R.G. Parr, Phys. Rev. B37 (1988) 785;
A.D. Becje, J. Chem. Phys. 98 (1993) 5648.
[20] G. Emmanual, C. Tenreaux, E.F. Queiroz, F. Zaila, M. Simonyi, S. Autus, A. Randriantsoa, K. Hosteltmann, Helv. Chemica. Acta 84 (2001) 3470.
[21] D. Zhang, X. Li, J. Kang, H. Choi, B. Son, Bull. Korean Chem. Soc. 28 (5) (2007) 887.
[22] R.I.H. Bayati, M.F. Radi, African J. Pure Appl. Chem. 4 (10) (2010) 228.
[23] T. Gonec, P. Bobal, J. Sujan, M. Pesko, J. Guo, K. Kralova, L. Pavlocka, L. Vesel, E. Kreckova, J. Kos, A. Coffey, P. Kollar, A. Imrmovsky, L. Placek, J. Jampilek, Molecules 17 (2012) 613.
[24] A. Magdy Ibrahim, M. Hany Hassanin, A. Yassin Gabr, A. Youssef Alnamer, J. Braz. Chem. Soc. 23 (5) (2012) 905.
[25] Gaussian 09, Revision A.1, M.J. Frisch, G.W. Trucks, H.B. Schlegel, G.E. Scuseria, M.A. Robb, J.R. Cheeseman, G. Scalmani, V. Barone, B. Mennucci, G.A. Petersson, H. Nakatsuji, M. Caricato, X. Li, H.P. Hratchian, A.F. Izmaylov, J. Bloino, G. Zheng, J.L. Sonnenberg, M. Hada, M. Ehara, K. Toyota, R. Fukuda, J. Hasegawa, M. Ishida, T. Nakajima, Y. Honda, O. Kitao, H. Nakai, T. Vreven, J.A. Montgomery, Jr., J.E. Peralta, F. Ogliaro, M. Bearpark, J.J. Heyd, E. Brothers, K.N. Kudin, V.N. Staroverov, R. Kobayashi, J. Normand, K. Raghavachari, A. Rendell, J.C. Burant, S.S. Iyengar, J. Tomasi, M. Cossi, N. Rega, J.M. Millam, M. Klene, J.E. Knox, J.B. Cross, V. Bakken, C. Adamo, J. Jaramillo, R. Gomperts, R.E. Stratmann, O. Yazyev, A.J. Austin, R. Cammi, C. Pomelli, J.W. Ochterski, R.L. Martin, K. Morokuma, V.G. Zakrzewski, G.A. Voth, P. Salvador, J.J. Dannenberg, S. Dapprich, A.D. Daniels, O. Farkas, J.B. Foresman, J.V. Ortiz, J. Cioslowski, D.J. Fox, Gaussian, Inc., Wallingford CT, 2009.